Final Draft
of the original manuscript:

Jepsen, J.; Milanese, C.; Girella, A.; Lozano, G.A.; Pistidda, C.; Bellosta von Colbe, J.M.; Marini, A.; Klassen, T.; Dornheim, M.:

Compaction pressure influence on material properties and sorption behaviour of LiBH4–MgH2 composite

In: International Journal of Hydrogen Energy (2013) Elsevier

DOI: 10.1016/j.ijhydene.2013.04.090

Compaction pressure influence on material properties and sorption behaviour of $LiBH_4$ - MgH_2 composite

Julian Jepsen[a,*], Chiara Milanese[b], Alessandro Girella[b], Gustavo A. Lozano[a], Claudio Pistidda[a], José M. Bellosta von Colbe[a], Amedeo Marini[b], Thomas Klassen[a], Martin Dornheim[a]

[a]Institute of Materials Research, Materials Technology, Helmholtz-Zentrum Geesthacht, Max-Planck-Strasse 1, D-21502 Geesthacht, Schleswig-Holstein, Germany
[b]Pavia H_2 Lab, Department of Chemistry, Physical Chemistry Division, University of Pavia, Viale Taramelli 16, I-27100 Pavia, Italy

Abstract

Among different Reactive Hydride Composites (RHCs), the combination of $LiBH_4$ and MgH_2 is a promising one for hydrogen storage, providing a high reversible storage capacity. During desorption of both $LiBH_4$ and MgH_2, the formation of MgB_2 lowers the overall reaction enthalpy. In this work, the material has been compacted to pellets for further improvement of the volumetric hydrogen capacity. The influence of compaction pressure on the apparent density, thermal conductivity and sorption behaviour for the Li-based RHC during cycling has been investigated for the first time. Although $LiBH_4$ melts during cycling, decrepitation or disaggregation of the pellets is not observed for any of the investigated compaction pressures. However, a strong influence of the compaction pressure on the apparent hydrogen storage capacity is detected. The influence on the reaction kinetics is rather low. To provide explanations for the observed correlations, SEM analysis before and after each sorption step was performed for different compaction pressures. Thus, the low hydrogen sorption in the first cycles and the continuously improving sorption for low pressure compacted pellets with cycling may be explained by some surface observations, along with the form stability of the pellets.

Keywords

Hydrogen storage, compaction, $LiBH_4$ - MgH_2, metal hydride, reactive hydride composites

1. Introduction

Metal hydride systems can be used as heat storage units [1], for gas purification [2] or pumping systems [3] or directly for hydrogen storage (e.g. [4-6]). There are several hydride systems applicable for energy storage by hydrogen. Beside sodium aluminium hydride ($NaAlH_4$) [4] and magnesium hydride (MgH_2) [7], the group of reactive hydride composite (RHC) is currently most interesting and could play a major role in the future [8]. In RHCs, two materials react exothermically with each other, and form a new compound while releasing hydrogen. Among different RHCs, the combination of lithium boron hydride ($LiBH_4$) and MgH_2 is one promising combination for hydrogen storage, providing a high storage capacity [9]. During desorption of both $LiBH_4$ and MgH_2, the exothermic formation of the new compound magnesium boride (MgB_2) lowers the overall reaction enthalpy [6, 10]:

$$2\ LiBH_4 + MgH_2 \rightleftharpoons 2\ LiH + MgB_2 + 4\ H_2 \qquad (1.1)$$

The theoretical maximum hydrogen capacity is 13.04 wt.% based on the desorbed state and 11.54 wt.% based on the absorbed state.
For larger bed sizes of hydride systems, the heat transport and not the intrinsic kinetics can limit the overall reaction rate. Considering the reaction described in equation 1.1, an energy of 46 kJ mol^{-1} H_2 is theoretically released or needs to be provided, for the absorption or desorption, respectively [9]. To provide solutions for this heat transport problem, the materials in previous studies were mixed with additives that improve the thermal conductivity (e.g. expanded natural graphite) [11-14]. Hence, the transformation rate was successfully enhanced, but with the drawback of a reduced volumetric and gravimetric capacity due to the addition of inert material.
In this work the material has been compacted to pellets as a start for further improvement of the volumetric hydrogen capacity. Beside the improvement of the volumetric capacity it is also expected that the compaction itself will lead to an improved thermal conductivity of the material.

*Corresponding author: tel.: +49 4152 87 - 2602; fax: +49 4152 87 - 2625
E-mail address: julian.jepsen@hzg.de (J. Jepsen)

The effect of the compaction is of particular interest for this system because, due to the melting of $LiBH_4$ [9] during the sorption process, decrepitation or disaggregation of the pellets is expected.

2. Experimental details

The desorbed state of the composite (right side of equation 1.1) has been chosen as initial material, and 5 mol-% of titanium chloride ($TiCl_3$) have been added as a reaction speed enhancer. The theoretical maximum hydrogen capacity, based on the desorbed state, is thus reduced to 10.9 wt.%. Lithium hydride (LiH; ≥ 99.4 % purity) and MgB_2 (99 % purity) were purchased from Alfa Aesar, the additive material $TiCl_3$ (≥ 99.995 % purity) was purchased from Sigma Aldrich. All the above quoted raw materials were purchased in powder form.
The materials have been processed in a planetary ball mill (Fritsch, Pulverisette 5, Germany) for 20 h with a ball to powder ratio of 10:1. After milling, the material was compacted at different pressures and diameters. For the compaction, a uniaxial manual hydraulic press (Specac, Manual Hydraulic Press, United Kingdom) with a maximum force of 15 ton has been used. The compaction was always performed in the same way: (i) The desired pressure was applied for 2 min.; (ii) the pressure was released for 1 min.; (iii) the desired pressure was again applied for another 2 minutes. To determine the apparent density as a function of the compaction pressure, different diameters, i.e. 5 mm, 8 mm, 10 mm, 13 mm and 20 mm, have been used, while for the sorption measurements only pellets of 5 mm and 8 mm in diameter were tested. The height of all pellets was at least 50 % and at most 150 % of the diameter, thus the weight of the pellets was not always the same. Different diameters for the sorption measurement were chosen to investigate the correlation between the diameter and the sorption rate. For the fitting of the apparent density against the compaction pressure, different diameters and the 3-steps procedure of compaction was chosen to minimise the error due to inhomogeneity in the density of the pellets, which is expected in particular for pellets with larger diameters. However, according to the literature, cross section observations by optical micrograph for different hydrogen absorption materials show no clear inhomogeneity for pellets up to 14 mm in diameter [14-16].
For the calculation of the thermal properties of the material, the Transient Plane Source (TPS) method [15, 16] has been applied. For the measurement a TPS 1500 system (C3 Prozeß- und Analysetechnik, Germany) has been used with a sensor of 13 mm in diameter. The applied power was between 100 and 350 mW. The measurements were performed at room temperature with a measurement time of 80 seconds. All handlings and measurements were carried out under Argon atmosphere in a glove box to avoid any atmospheric impurities.
The sorption rate was measured using a Sievert's apparatus (HERA, Canada) based on the differential pressure method. The purity of the used hydrogen gas was 5.0 (99.999 %). The measurements conditions were 350 °C and 50 bar hydrogen for the absorption and 400 °C and 5 to 2 bar of hydrogen for the desorption.
The observations by scanning electron microscope (SEM) have been performed with an EvoMA10 (Zeiss, Germany) microscope equipped with a LaB_6 filament for x-ray analysis. The composition of the samples is determined by Energy Dispersion Microanalysis (EDS), using an INCA Energy 350 X Max detector from Oxford Instruments, equipped with a Be window. Cobalt standard is used for the calibration of the quantitative elementary analysis. To avoid oxidation during the handling of the sample, a special sample holder was used. Thereby the sample was placed inside the glove box in the sample holder and afterwards a vacuum was created inside the holder to transport the sample to the SEM.

3. Results

3.1. Initial density and thermal conductivity

Initially, and as a reference, the loose powder density of the desorbed material was determined at 0.6243 ± 0.018 g cm^{-3} by using a defined volume and measuring the mass of the powder that fits inside without compacting it. The maximum density was calculated theoretically by using the crystalline solid density and the molar mass of the two components LiH and MgB_2 for the desorbed state and $LiBH_4$ and MgH_2 for the absorbed state (Tab. 1).

Material	Solid density ρ [g/cm^3]	Molar mass M [g/mol]	Reference
$LiBH_4$	0.66	21.78	[17, 18]
LiH	0.82	7.95	[19]
MgB_2	2.57	45.93	[18]
MgH_2	1.45	26.32	[19]

Table 1: Solid density and molar mass of the different components in absorbed and desorbed state

The stoichiometric composition of the desorbed and absorbed material follows the simplified reaction equation 1.1 [9]. For this equation and for the calculation of the maximum density, the addition of $TiCl_3$ was neglected.
The maximum density was calculated to be 0.83 g cm^{-3} for the absorbed state and 1.66 g cm^{-3} for the desorbed state, which was defined, for practical purposes, as zero point of the porosity. Following this definition, the porosity of the loose desorbed powder material could be calculated to be around 65 %. As can be seen in figure 1, the apparent density clearly increases with increasing compaction pressure. The change in apparent density and porosity is strong at the beginning of the compaction process up to approximately 50 MPa and levels off at higher pressures towards the maximum i.e. solid density of the desorbed state. The trend of the apparent density curve is similar to other hydride systems like MgH_2 [11] or $NaAlH_4$ [12].

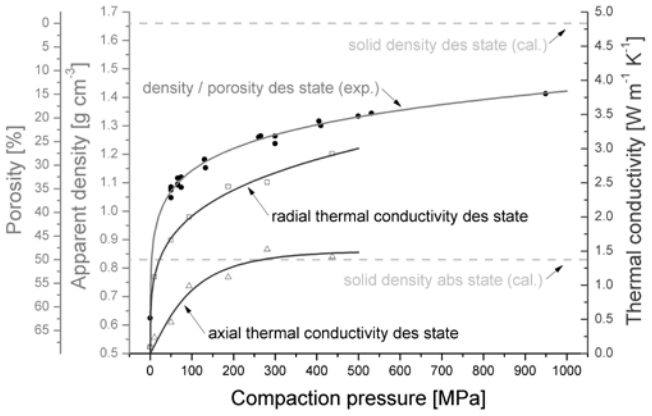

Fig. 1: Apparent density / Porosity and thermal conductivity in axial and radial direction against compaction pressure of the desorbed state of the material (LiH / MgB_2)

The increase in apparent density and decrease in porosity of the initial desorbed material affects also the thermal conductivity of the pellet. The relatively poor thermal conductivity of the material in the loose powder state of ~0.1 W m^{-1} K^{-1} increases with the apparent density. This correlation is independent from the direction of the thermal conductivity. However, the rate of increase is different. As seen in figure 1 the influence of the change in apparent density on the radial thermal conductivity is greater then on the axial one. Additionally it seems that the axial thermal conductivity reaches a maximum value after 300 MPa compaction pressure while the radial conductivity still increases above this value.
All these property changes can be observed for the initial powder (desorbed state) at room temperature and under Argon atmosphere. Due to the absorption and desorption reaction and the related temperature and hydrogen pressure these properties might change again.

3.2. Kinetic and hydrogen capacity

To show the effect of compaction on hydrogen capacity and kinetics, four different samples have been compacted at 600 MPa (sample 1), 300 MPa (sample 2), 150 MPa (sample 3) and 75 MPa (sample 4). The samples have absorbed and desorbed hydrogen for 4 cycles and they are compared to an uncompacted sample that was cycled in the same way (sample 5). The comparison of the 4th absorption and desorption is shown in figure 2. The absorption of the compacted specimens stagnates at different fractions of the regular capacity of the loose powder. Thus, the compaction pressure clearly influences the final absorbed capacity. Starting at approximately 9 wt.% for the uncompacted loose powder, the final capacity decreases with increasing compaction pressure, reaching only 2 wt.% for 600 MPa compaction pressure. The absorption rate correlates with the compaction pressure in the same way. In contrast, the desorption rate is similar for all compaction pressures.

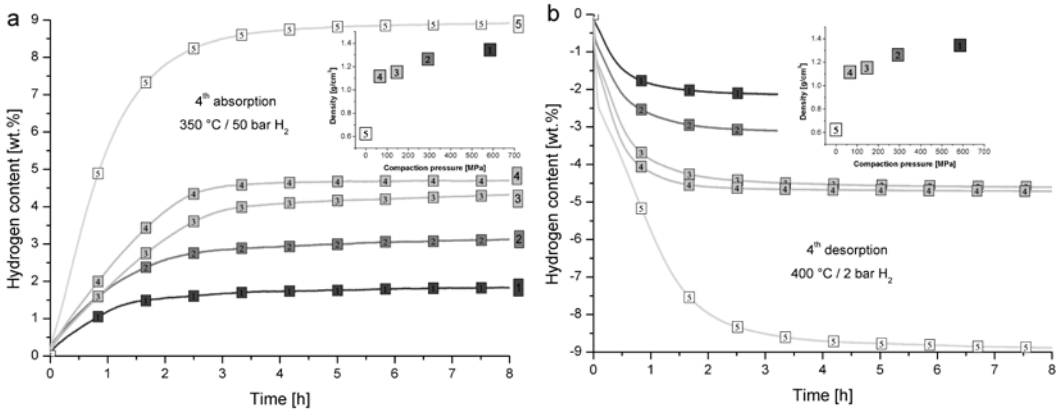

Fig. 2: Hydrogen content against time of the 4th absorption at different compaction pressures at 350 °C and 50 bar H_2 during absorption (a) and 400 °C and 2 bar H_2 during desorption (b)

The lost capacity can be regained with increasing number of cycles. For example for a compaction pressure of 75 MPa (comparable to sample 4 in figure 2), the maximum regular capacity at around 9 wt.% is reached after 9 cycles (Fig. 3). As for the loose powder, the kinetics of the first absorption is sluggish also for the compacted sample (e.g. [6]). Afterwards, the capacity and also the kinetics increase from cycle to cycle with the exception of the second cycle. For the second cycle the capacity drops uniquely under the capacity of the previous first cycle. This behaviour of the second cycle was also observed for other compacted and uncompacted samples (see also Fig. 5). The system is fully reversible and desorbs the full amount that was previously absorbed (Fig. 3b).

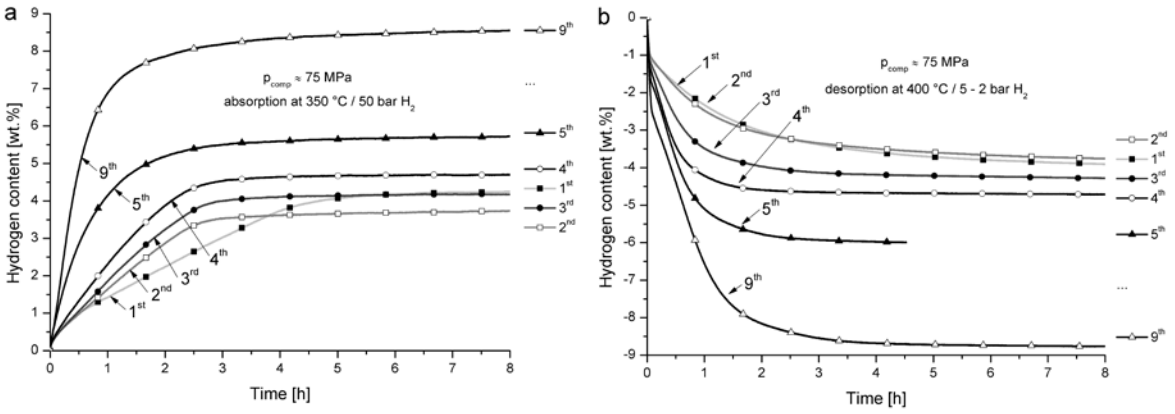

Fig. 3: Hydrogen content against time of different cycles at 75 MPa compaction pressures at 350 °C and 50 bar H_2 during absorption (a) and 400 °C and 5-2 bar H_2 during desorption (b)

Beside the capacity, also the kinetics of the compacted sample after 9 cycles is in good agreement with a cycled loose powder sample (Fig. 4). In this figure, the 9th absorption and desorption of a compacted sample are compared to an 8th absorption and a 4th desorption of an uncompacted sample, respectively. The 9th cycle of the compacted sample has been chosen because of the fact (see figure 3) that it takes at least 9 cycles at this compaction pressure until the material reaches its complete capacity. The comparison to an 8 times cycled loose powder sample for absorption and an only 4 times cycled sample for the desorption have been made because it is know from previous works that

the influence of the cycles on the absorption is strong while there is almost no influence on the desorption [20].

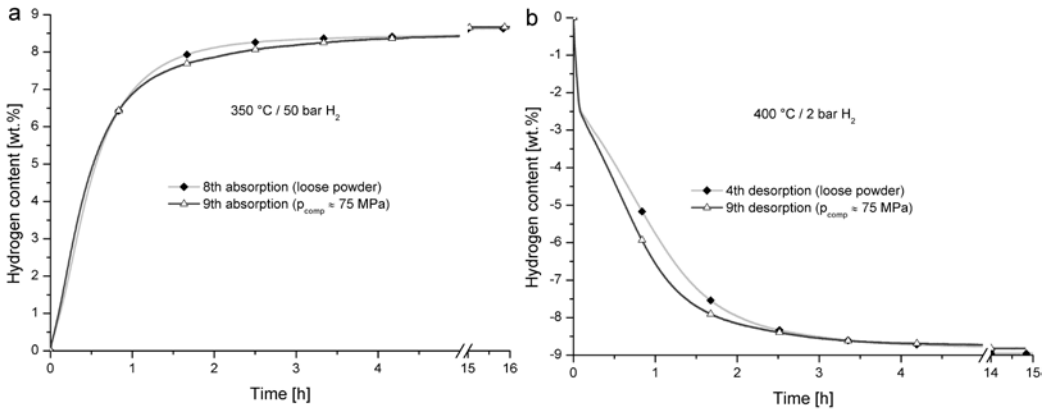

Fig. 4: Hydrogen content against time of compacted and uncompacted sample at 350 °C and 50 bar H_2 during absorption (a) and 400 °C and 2 bar H_2 during desorption (b)

In figure 4 it can be noted that the compaction of the material and the consequent initial improvement of the volumetric capacity (Fig. 1) has no negative influence on the kinetics of the material during the absorption and desorption processes. The influence on the capacity can be summarised with figure 5a: a lower compaction pressure leads to higher capacities and upon cycling, capacities comparable to loose powder systems can be reached faster. This depends, besides the compaction pressure, also on the geometry of the pellet. The so far shown measurements have been performed with pellets of 8 mm in diameter. Comparable measurements with 5 mm pellets show a similar behaviour. However, capacities approach the loose powder capacity faster for a given compaction pressure (Fig. 5a).
Fig 5b indicates, that the decrease in capacity upon cycling is less pronounced for compacted specimen in comparison to loose powder beds ($m_{MATERIAL} \leq 150$ mg). A possible explanation could be that the degradation of the capacity is due to increasing segregation of the reaction partners upon cycling, which may be less pronounced in compacted material.

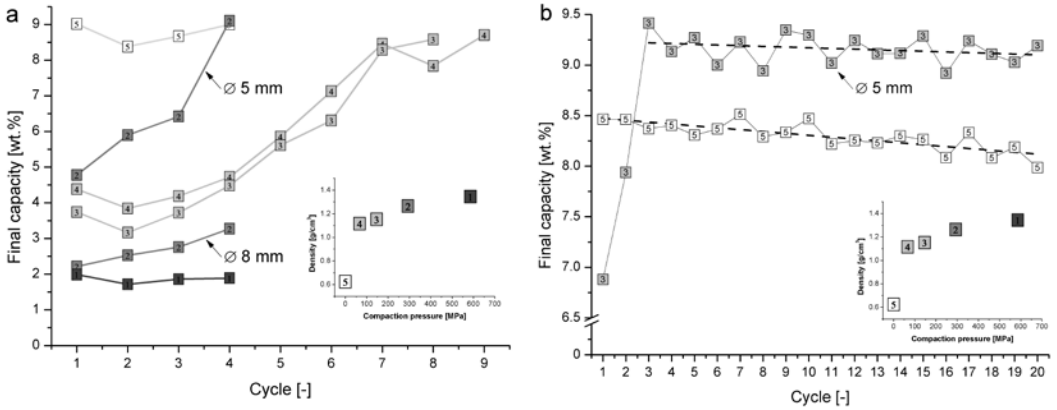

Fig. 5: Final hydrogen capacity after absorption at 350 °C and 50 bar H_2 for different compaction pressures and dimensions for maximum 9 cycles (a) and over 20 cycles (b)

3.3. Surface morphology

The increase in capacity during cycling of the compacts may be related to crack formation and disintegration of the compacts. Furthermore, morphology changes could be expected due to the phase transformation from solid LiH to liquid $LiBH_4$ during cycling, which may also change the apparent density and the correlated volumetric capacity. Therefore, the pellets and in particular their surface morphology was investigated.

For the influence of the compaction pressure on the surface morphology upon cycling, three different compaction pressures have been investigated: lightly (50 MPa), medium (300 MPa) and high (950 MPa). The initial diameter of each specimen was ~5 mm and the height roughly the same. The samples were cycled four times with four complete absorption and desorption runs under the standard reaction conditions of 350 °C and 50 bar for absorption and 400 °C and 5 to 2 bar for desorption. After each sorption, a "macroscopic" SEM image was taken to observe the shape of the complete diameter or shell. After the 3rd absorption and the 3rd desorption respectively, additionally "microscopic" SEM images were taken to observe the surface morphology in detail with a magnification of 300 to 5,000. The results of the kinetics and hydrogen capacity tests with these pellets were in agreement with previous ones, as shown in paragraph 3.2: the lightly compacted sample reaches the full capacity (9 wt.%) within 3 cycles and the medium compacted within 4 (sample 2 (5 mm) in Fig 5). The highly compacted sample absorbed only a few weight percent, even after 4 cycles (comparable to sample 1 in Fig. 5).

In figure 6 the macroscopic surface of the lightly compacted pellet is shown in radial direction (complete diameter) upon cycling. The effect of the first sluggish absorption on the surface morphology is rather small in comparison to the subsequent sorption reactions. After the first desorption the formation of cracks and fractures on the surface is clearly visible in this radial view.

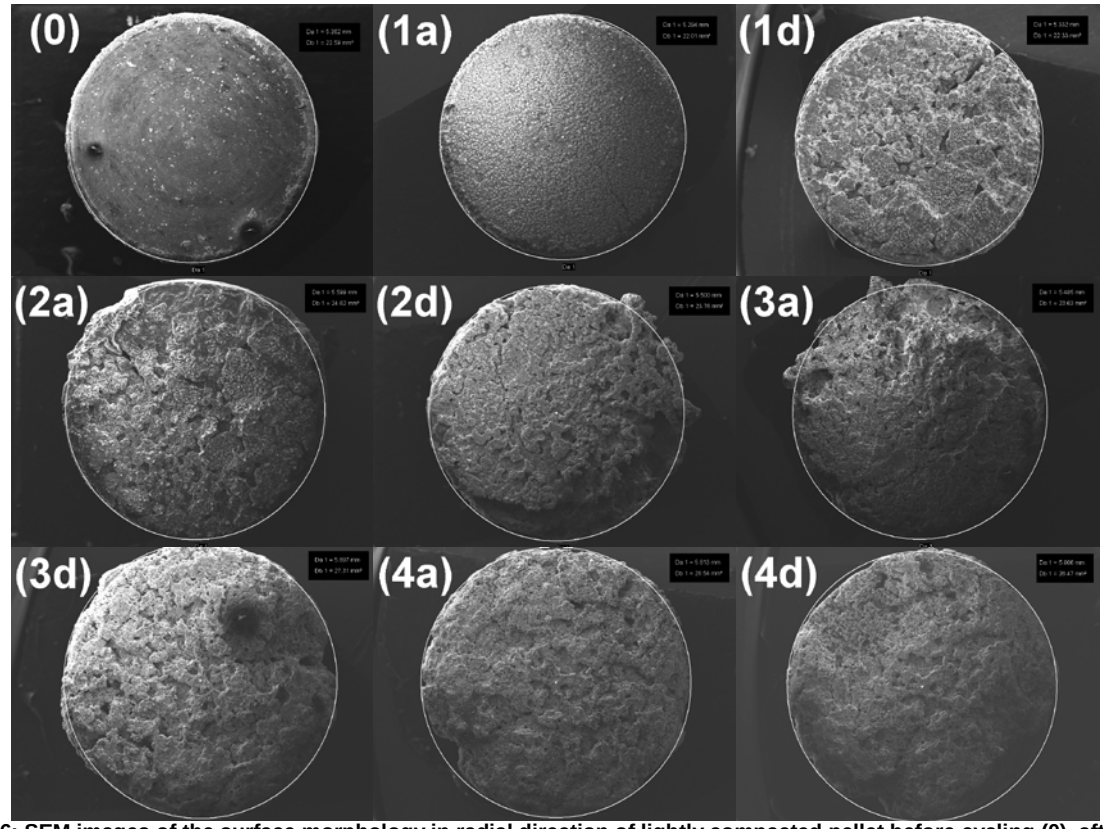

Fig. 6: SEM images of the surface morphology in radial direction of lightly compacted pellet before cycling (0), after 1st abs. (1a), 1st des. (1d), 2nd abs. (2a), 2nd des. (2d), 3rd abs. (3a), 3rd des. (3d), 4th abs. (4a) and 4th des. (4d)

The upper surface of the pellet remains mostly in a circular shape in this view, but the overall expansion and change of the shape of the sample is clearer in the axial direction (shell) for the lightly compacted sample (Fig. 7a). The initial 4.70 mm height grows to 5.91 mm (+25.8 %) while the diameter changes from 5.362 mm to 5.806 mm (+8.3 %) after 4 cycles. The expansion is irregular and asymmetric. The apparent density changes thus from the initial 0.94 g cm^{-3} to 0.64 g cm^{-3} (+32.2 %).

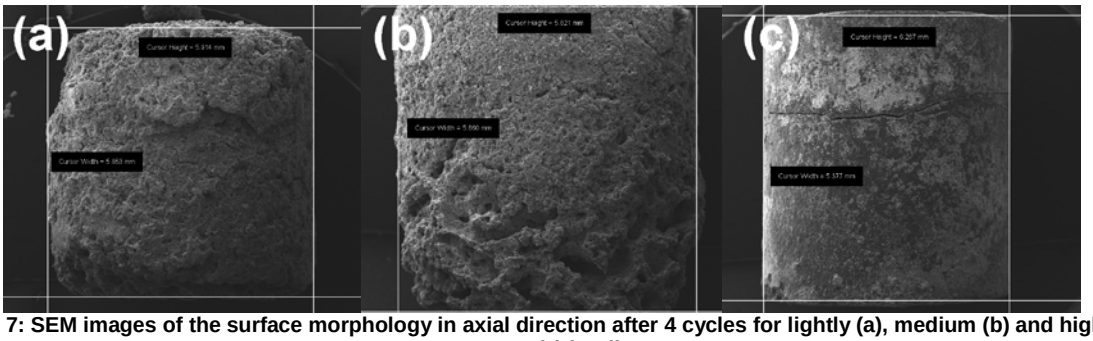

Fig. 7: SEM images of the surface morphology in axial direction after 4 cycles for lightly (a), medium (b) and highly compacted (c) pellets

The same swelling can be observed for the medium compacted sample (Fig. 7b) even though the growing is less extensive in comparison to the lightly compacted sample after four cycles (height change: from 4.65 mm to 5.82 mm, +25.2 %; diameter change: from 5.362 mm to 5.660 mm, +5.6 %; apparent density change: from 1.09 g cm^{-3} to 0.79 g cm^{-3}, +28.3 %). The expansion of the highly compacted sample (Fig 7c) is clearly lower and the pellet keeps its cylindrical shape in axial but especially in radial direction almost completely (height change: from 5.60 mm to 6.34 mm, +13.2 %; diameter: from 5.378 mm to 5.474 mm, +1.8 %; apparent density: from 1.22 g cm^{-3} to 1.04 g cm^{-3}, +14.7 %).

The microscopic SEM observation for the lightly compacted sample after the 3rd absorption using two different magnification settings (500x and 1500x) is shown in figures 8a and 8b. As a comparison, an uncompacted loose powder sample after the 3rd absorption (Fig. 8c and 8d) and the 3rd desorption (Fig. 8e and 8f lightly compacted and 8g and 8h uncompacted) are also shown. The porous structure of the pellet after cycling with many cracks and holes (Fig. 8a and 8e) can be clearly distinguished from the loose particle structure of the uncompacted sample (Fig. 8c and 8g) after absorption and desorption. A closer examination on the compacted sample reveals small areas with very smooth surfaces homogeneously dispersed, which may be related to the solidification of a liquid phase. After desorption (Fig. 8f) these features have almost disappeared and only a porous solid matrix is visible.

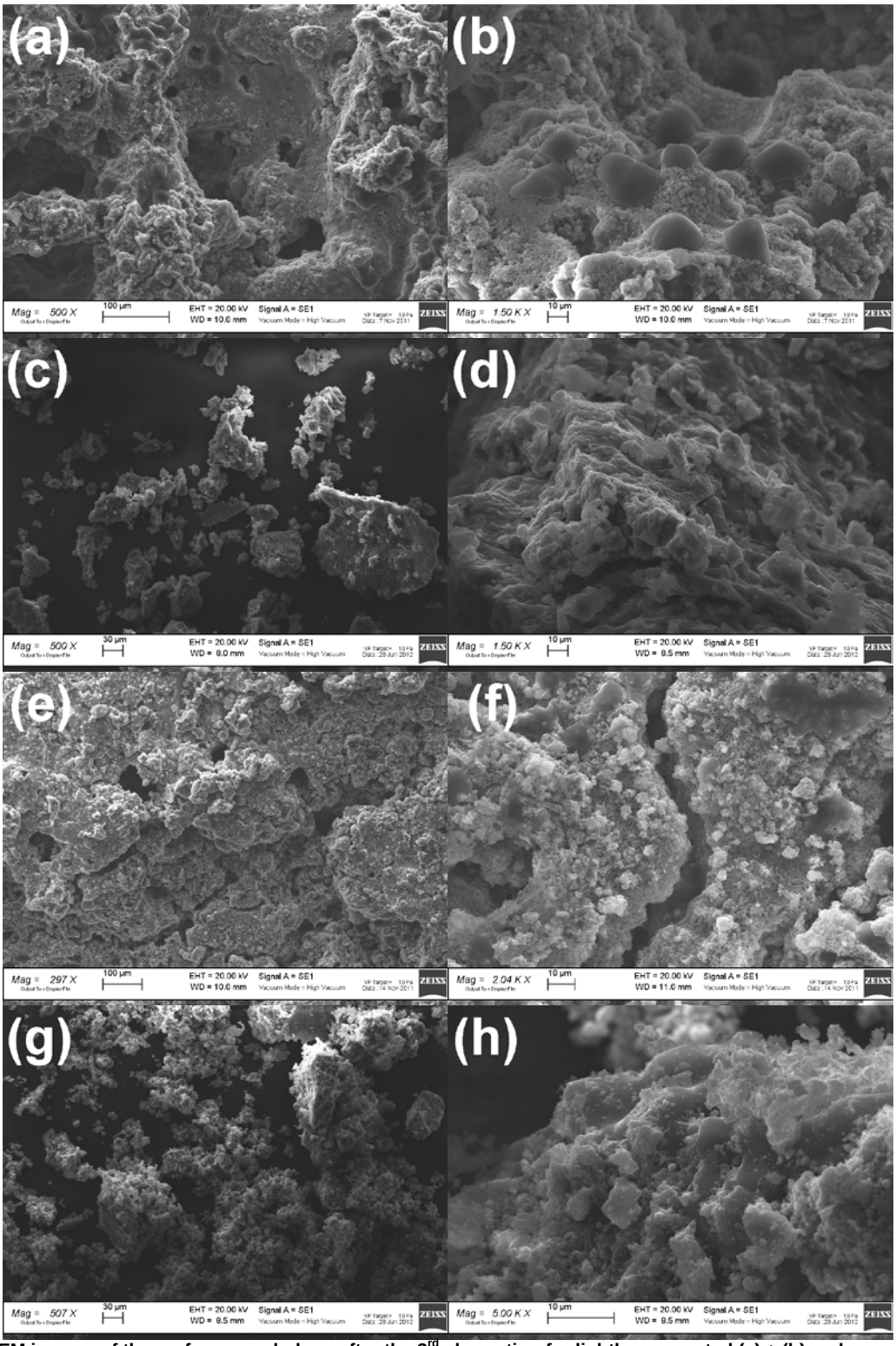

Fig. 8: SEM images of the surface morphology after the 3rd absorption for lightly compacted (a) + (b) and uncompacted sample (c) + (d) and after the 3rd desorption for lightly compacted (e) + (f) and uncompacted sample (g) + (h)

4. Discussion

The above mentioned changes in diameter and height are shown as relative change also for the density in figure 9. The density is calculated according to the measured height and diameter after 4 cycles. Calculation for the lightly and medium compacted samples is hindered by the irregular and asymmetric expansion and therefore just seen here as a rough estimation. As described in paragraph 3.3, the change in height is greater than the change in diameter by a factor of 3 to 4.5. This is comparable to pellets made of pure MgH_2 were the axial expansion is mentioned in literature to be 3 times greater than the radial expansion [21]. The reason for the asymmetric expansion may be directional recrystallisation of the hydride but is still not well understood [21, 22]. The higher dimensional change in height could also be explained by the uniaxial compaction, where the force in axial direction is higher and therefore also the deformation. This may lead to texturing.

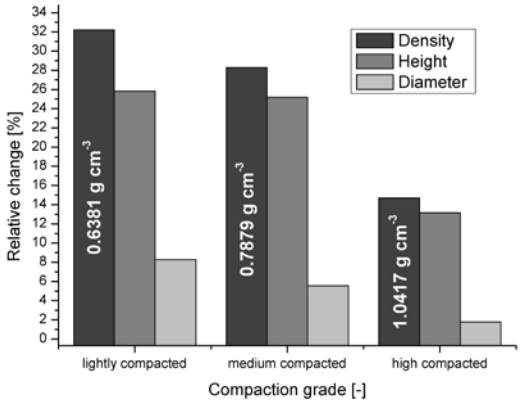

Fig. 9: Change of the geometrical density, height and diameter for a low, medium and high compacted pellet after 4 cycles

Interestingly, the initial hydrogen capacities of the compacts are significantly lower than the capacities of loose powder beds. Upon cycling, the capacity is gradually regained. The lightly and medium compacted samples reach their full capacity of 9 wt.% after 4 cycles, while the highly compacted samples reach only less then 2 wt.% hydrogen storage capacity after 4 cycles. Moreover the recovery of the full capacity is faster upon further cycling for pellets with smaller diameters.
In principle, this could be explained by two different reasons:
(i) As described in paragraph 3.2 (e.g. in Fig 2 and 3) high stresses may develop between a hydrogen absorbing region of the compact and the adjacent unhydrided material, in particular in the highly compacted samples (≥ 600 MPa), which may suppress the hydriding reaction. These stresses will be reduced during the cycling due to the expansion of the pellets, which can explain the improvement of the hydrogen capacity upon cycling.
(ii) The highly compacted material may reach a state of closed porosity after compaction and the other compacts would reach this state at higher hydrogen levels due to the concomitant swelling. Then, hydrogen gas would have no direct access to the core of the compacted cylinders. The outside shell of the pellet would be hydrided first, and this hydrided shell would effectively block diffusion of hydrogen to the core. E.g., the diffusion coefficient of hydrogen in MgH_2 [23] is lower by a factor of 5,000 as compared to the pure unhydrided Mg [24, 25]. Then, further hydrogen uptake would be unrecognisable in the given time for the measurement. Upon desorption, cracks would form and, during cycling, the respective expansion and crack formation would gradually increase the depth that is quickly accessible to hydrogen gas.
Finally the main cause for the approaching of the loose powder capacities in the two above described theories is the volumetric expansion and the consequent formation of cracks and defects. For pellets with smaller diameter, the whole volume is accessible sooner, if constant crack growth towards the centre of the pellet is assumed upon cycling. This would explain the faster recovery of the capacity for pellets made of smaller diameters.
To elucidate this point and to compare the residual porosities, Fig. 10 shows the experimentally determined densities for the respective measured capacities of the samples 1 to 5 after the first absorption. Fitting of these points gives a perfect straight line that falls below the line for the theoretical density, which is calculated based on the solid density of the desorbed state (1.66 g cm^{-3}) and the maximum capacity (9 wt.%) for the solid density of the absorbed state (0.83 g cm^{-3}), and assuming a direct correlation between the phase fraction of the hydrided phase and the hydrogen capacity. The gap between these lines represents the residual porosity of the pellets. This porosity is reduced with high compaction pressure and, thus, the distance between the two lines is less for high densities. The

residual porosity for the highly compacted specimen is about 10 %, which is indeed around the limits for closed porosity and can explain the low capacities in the first cycles, as well as the gradual improvement upon gradual expansion.

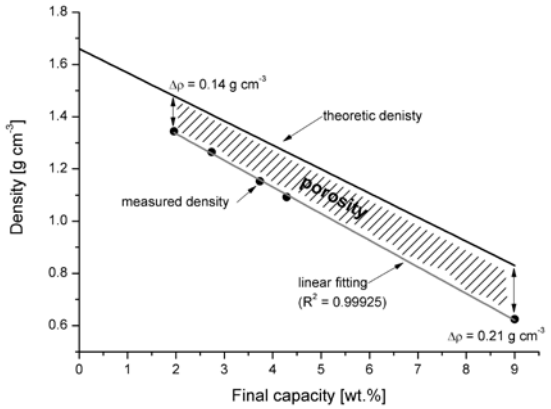

Fig. 10: Gap between measured density and theoretical density for the given capacities after the first absorption.

Even though the initial improvement of the volumetric density gradually decreases and is almost lost according to the final densities in figure 9, the pellets still retain their cylindrical shape. The reason why the pellets do not decrepitation or disaggregate, in particular after absorption, may be the framework that can be seen in figure 8a. The framework presumably consists mainly of the solid Mg – compounds, and after absorption in particular MgH_2, by assuming that the small and well dispersed particles with the smooth surface are consisting of $LiBH_4$, that was liquid during the reaction and solidified on the MgH_2 lattice after cooling down. In this sense, the Mg - compounds act as shape-retainer. Unfortunately, this theory could not be proven yet by local EDX analysis, because lithium and boron atoms are too light and the only atoms detected were magnesium and some small amounts of oxides.

The initially improved thermal conductivity with higher apparent densities by increased compaction pressure can be explained by the reduced porosity and the improved thermal contact between the powder particles. The different behaviour of the axial and radial thermal conductivity can moreover be explained by the uniaxial compaction. Due to this compaction, the particles are compressed together preferentially in the axial direction and to a lesser extent in radial direction. Therefore, the thermal conductivity is improved in the radial direction due to the alignment of larger particles in this direction. In addition, the uniaxial compression results in a high density of interfaces between different phases in axial direction, which limit heat transfer. In contrast, the predominantly elongated single-phase particles in the radial direction provide better heat transfer.

The thermal conductivity will be reduced during cycling due to the expansion and the resulting lower density, but the above mentioned Mg - compound framework may still facilitate reasonably high thermal conductivity. Unfortunately, this effect could not be measured because the method used in this work needs perfect thermal contact on the sensor / sample interface. Due to the porosity and irregular surfaces generated during cycling, this contact could not be ensured.

Even though the improvement of the volumetric density and thermal conductivity is gradually lost during cycling, capacity (after some cycles) and kinetics are as good as for loose powder and the long time cycling stability can even be improved. Obviously, segregation of the reactants is avoided by compaction and the formation of an Mg-based framework. An additional advantage of compaction is that handling of compacts in the tank manufacture process is much safer than using loose powders.

5. Conclusion

In this work, the influence of the compaction on density, thermal conductivity and sorption behaviour for the Li-based RHC during cycling has been investigated. A strong influence of the compaction pressure on the accessible hydrogen storage capacity is found as well as a slight influence on the kinetics. The low hydrogen sorption in the first cycles and the continuously improving sorption with cycling can be explained either by the suppression of the necessary expansion with increasing hydrogen content or by the sluggish access of hydrogen to the core of the compact by a dense layer of hydrided phase forming on the outer shell. The compacts recover the maximum hydrogen capacity gradually over cycling, but loose their initial improvement in volumetric density concomitantly. Nevertheless, and although $LiBH_4$ melts during cycling, complete decrepitation or disaggregation of

the pellets, as well as segregation of the RHC components, is not observed for any of the investigated compaction pressures. The observed form stability of the pellets may be explained by a stable framework of solid Mg – compounds, i.e. MgB_2 or MgH_2, respectively. Thus, the results indicate, that compaction may be a possible way to solve problems related to segregation of the reaction partners in RHCs.

6. Outlook

The ongoing work will be focused in particular on the scaling effect of the compaction and will show, whether this influence is also present for larger diameters like 60 mm and more. Beside a possibly negative influence by larger diameters on the kinetics, there may still be a positive influence by the improved thermal conductivity, because with increasing sample size the importance of thermal conductivity should also increase.

Acknowledgments

The authors appreciate the partial financial support of the DAAD (German Academic Exchange Service) in the frame of the Project “VIGONI”.

Reference

[1] Koseki, Takami, Takeda, Harunobu, Lijima, Kazuaki, et al. Development of heat-storage system using metal hydraid: Experiment of performance by the actual loading condition. New York, NY, ETATS-UNIS: American Society of Mechanical Engineers; 2006.

[2] Rudman PS, Sandrock GD, Goodell PD. Hydrogen Separation from Gas-Mixtures Using Lani5 Pellets. Journal of the Less-Common Metals. 1983;89:437-46.

[3] Kim KJ, Feldman Jr KT, Lloyd G, Razani A. Compressor-driven metal-hydride heat pumps. Applied Thermal Engineering. 1997;17:551-60.

[4] Bogdanovic B, Schwickardi M. Ti-doped alkali metal aluminium hydrides as potential novel reversible hydrogen storage materials. Journal of Alloys and Compounds. 1997;253:1-9.

[5] Barkhordarian G, Klassen T, Dornheim M, Bormann R. Unexpected kinetic effect of MgB2 in reactive hydride composites containing complex borohydrides. Journal of Alloys and Compounds. 2007;440:L18-L21.

[6] Vajo JJ, Skeith SL, Mertens F. Reversible Storage of Hydrogen in Destabilized LiBH4. J Phys Chem B. 2005;109:3719-22.

[7] Barkhordarian G, Klassen T, Bormann R. Kinetic investigation of the effect of milling time on the hydrogen sorption reaction of magnesium catalyzed with different Nb2O5 contents. Journal of Alloys and Compounds. 2006;407:249-55.

[8] Barkhordarian G, Klassen T, Bormann R. Patent pending, German Pub. No: DE102004/061286. 2004.

[9] Bösenberg U, Doppiu S, Mosegaard L, Barkhordarian G, Eigen N, Borgschulte A, et al. Hydrogen sorption properties of MgH2-LiBH4 composites. Acta Materialia. 2007;55:3951-8.

[10] Dornheim M, Eigen N, Barkhordarian G, Klassen T, Bormann R. Tailoring hydrogen storage materials towards application. Advanced Engineering Materials. 2006;8:377-85.

[11] Chaise A, de Rango P, Marty P, Fruchart D, Miraglia S, Olivès R, et al. Enhancement of hydrogen sorption in magnesium hydride using expanded natural graphite. International Journal of Hydrogen Energy. 2009;34:8589-96.

[12] Lozano GA, Bellosta von Colbe JM, Bormann R, Klassen T, Dornheim M. Enhanced volumetric hydrogen density in sodium alanate by compaction. Journal of Power Sources. 2011;196:9254-9.

[13] Kim KJ, Montoya B, Razani A, Lee KH. Metal hydride compacts of improved thermal conductivity. International Journal of Hydrogen Energy. 2001;26:609-13.

[14] Pohlmann C, Röntzsch L, Kalinichenka S, Hutsch T, Kieback B. Magnesium alloy-graphite composites with tailored heat conduction properties for hydrogen storage applications. International Journal of Hydrogen Energy. 2010;35:12829-36.

[15] Gustafsson SE, Karawacki E, Khan MN. Transient hot-strip method for simultaneously measuring thermal conductivity and thermal diffusivity of solids and fluids. Journal of Physics D: Applied Physics. 1979;12:1411.

[16] Al-Ajlan SA. Measurements of thermal properties of insulation materials by using transient plane source technique. Applied Thermal Engineering. 2006;26:2184-91.

[17] Züttel A, Wenger P, Rentsch S, Sudan P, Mauron P, Emmenegger C. LiBH4 a new hydrogen storage material. Journal of Power Sources. 2003;118:1-7.

[18] Lide DR. Handbook of Chemistry and Physics. London: CRC Press; 1994.

[19] Sitzmann H. Römpp Online. Thieme Verlag.

[20] Bösenberg U. LiBH4-MgH2 composites for hydrogen storage. Hamburg/Germany: Technische Universität Hamburg-Harburg; 2009.

[21] Delhomme B, de Rango P, Marty P, Bacia M, Zawilski B, Raufast C, et al. Large scale magnesium hydride tank coupled with an external heat source. International Journal of Hydrogen Energy. 2012;37:9103-11.

[22] Khandelwal A, Agresti F, Capurso G, Lo Russo S, Maddalena A, Gialanella S, et al. Pellets of MgH2-based composites as practical material for solid state hydrogen storage. International Journal of Hydrogen Energy. 2010;35:3565-71.

[23] Renner J, Grabke H. Determination of diffusion coefficients in the hydriding of alloys. Zeitschrift für Metallkunde. 1978;69:639-42.

[24] Töpler J, Buchner H, Säufferer H, Knorr K, Prandl W. Measurements of the diffusion of hydrogen atoms in magnesium and Mg2Ni by neutron scattering. Journal of the Less Common Metals. 1982;88:397-404.

[25] Stander CM. Kinetics of formation of magnesium hydride from magnesium and hydrogen. Zeitschrift Fur Physikalische Chemie-Frankfurt. 1977;104:229-38.